Accuracy of Activation Times Detected in Simulated Extracellular Electrograms

FB Sachse[1], G Seemann[2], DL Weiß[2], BB Punske[1], B Taccardi[1]

[1]Nora Eccles Harrison Cardiovascular Research and Training Institute, University of Utah, USA
[2]Institut für Biomedizinische Technik, Universität Karlsruhe (TH), Germany

Abstract

Detection of local activation times is a basic operation in cardiac electrophysiological research and applied for several analysis techniques. Conduction velocity can be determined by the difference of activation times at two positions divided by their spatial distance. In this work the accuracy of activation time detection was analyzed in a modeling study of papillary muscle surrounded by a bath. An electrophysiological model of the muscle was developed and a numerical simulation was performed. The simulation yielded spatiotemporal distributions of transmembrane and extracellular voltages, which were used to detect activation times. The study indicated that the relationship between longitudinal distance of measurement position and detected activation time is mostly nonlinear, particularly at both ends of muscle. Thus, conduction velocity can be detected with a given accuracy only in a specific area in-between, which is defined by geometrical relationships.

1. Introduction

A fundamental analysis operation in studies of cardiac electrophysiology is the extraction of local activation times. In numerous studies this operation was applied e.g. to create activation and isochrone maps as well as to determine conduction velocity. While detection of activation times in transmembrane voltage recordings is possible with simple numerical methods, detection in extracellular electrograms is challenging due to interferences from non-related electrical sources and a commonly significantly smaller signal-to-noise ratio. Further complexity is added by geometrical relationships between the positions of the measurement electrodes, the activation front and its spatial domain.

Aim of this computational study was to quantify the accuracy of activation time detected in extracellular electrograms considering the geometrical relationships. An electrophysiological model of papillary muscle in a bath was studied. Papillary muscles are frequently used to characterize electrical properties of myocardium and conduction velocity under varying experimental conditions.

This computational study parallels an experimental study of mechano-electrical feedback mechanisms in papillary muscle. A crucial component of analysis in this experimental study is the accurate detection of activation times. The computational study was designed to reproduce experimental conditions, where a stimulus is given at one end of the preparation and electrograms are acquired at some points along its surface. The relationship between activation times detected extracellularly and from the transmembrane voltage at these points and related points in the muscle, respectively, was investigated.

2. Methods

2.1. Experimental conditions

In previous work we developed a software-controlled experimental setup for studying cardiac mechano-electrical feedback [1]. In short the setup allows measurement of extracellular electrograms originating from papillary muscle. The measurement procedure is automated and necessitates only minor user interaction (Fig. 1).

The software reads and controls a motorized micromanipulator (MP-285, Sutter Instrument Company, CA) via a serial interface for positioning of a recording electrode and measuring of muscle geometry. Furthermore, electrical data were acquired with a sampling rate of $10\ kHz$ via a multi-function data acquisition card (PCI-6031E, National Instruments Corporation, TX). The digital input of this board was employed to read triggering signals from the stimulator. Electrograms were recorded via a silver wire of diameter of $150\ \mu m$. The wire was fully insulated except at the tip, which was chlorided. The electrodes were attachable by a rod to the motorized micromanipulator. The stimulus electrodes were made of silver wire with a diameter of $150\ \mu m$ and positioned by a manual manipulator. A stimulus frequency of $0.5\ Hz$ was chosen.

Electrical signals were acquired from a set of positions, which were determined from a set of points given by the user through steering a pointer with the motorized

0276–6547/04 $20.00 © 2004 IEEE

Computers in Cardiology 2004;31:93–96.

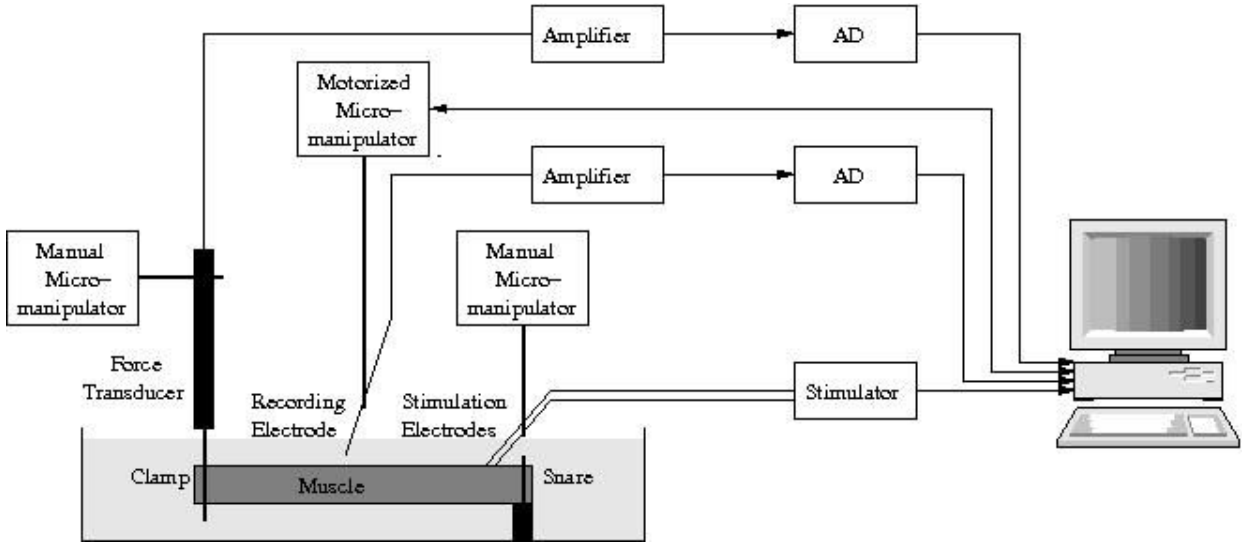

Figure 1. Sketch of measurement setup (modified from [1]). The muscle is placed in a horizontal flow-through chamber filled with a modified Tyrode solution of temperature of 37^oC. The muscle is fixed rigidly on the right side with a snare. On the muscle's left side a clamp attached via a force transducer to a micro-manipulator provides fixation. The stimulus is applied in proximity to the snare fixed end of muscle. The reference electrode is located at the left end of the bath.

manipulator. The coordinates of these points were read digitally from the manipulator. Commonly, the recording electrode served as pointer and points at the ends of the muscle were selected. The given coordinates were applied to describe line segments or quadrangles, which were discretized using sampling of finite element shape functions [2].

2.2. Computational model

A computational model was created to mirror relevant aspects of the previously described experimental setup. Central component of the model was a bidomain description used to reconstruct excitation propagation as well as the corresponding intra- and extracellular potential distribution [3].

The bidomain model based on a simplified geometrical description of the papillary muscle, the bath, and the reference electrode. The model included anisotropic intra- and extracellular conductivities as well as a biophysically based cellular electrophysiological model, i.e. the Noble-Kohl-Varghese-Noble model of a ventricular myocyte [4]. For both domains the generalized Poisson's equation for electrical current fields was applied, which was discretized with the finite element method on hexahedral grids consisting of 45 x 45 x 70 elements in x-, y-, and z-direction. Each element was cubic with an edge length of 100 μm. A cylinder with a radius of 1 mm and a length of 3 mm was rendered in both grids to represent the papillary muscle. The long axis of the cylinder was parallel to the z-axis.

The following conductivities were chosen (in S/m): myocardium extracellular longitudinal $\sigma_{e,l} = 0.2$ and transversal $\sigma_{e,t} = 0.0666$, myocardium intracellular longitudinal $\sigma_{i,l} = 0.2$ and transversal $\sigma_{i,t} = 0.0333$, and bath $\sigma_b = 1$.

2.3. Data analysis

The activation time in computed courses of transmembrane voltages and extracellular electrograms was detected by searching for the maximal and minimal temporal derivative, respectively [5, 6]. The search was restricted to a time window after the stimulation to neglect thereby caused artifacts.

3. Results

The spread of excitation through the papillary muscle was simulated and visualized (Figs. 2 and 3). A stimulus current was applied extracellularly at $t = 0.5\ ms$ for a length of $1\ ms$ at the center of the right face of the muscle. Dirichlet boundary conditions were defined on the left side of the bath setting the extracellular potential to zero. The simulation described a duration of $20\ ms$.

In initial phases of excitation conduction a high curvature of the propagation front was found followed by a decrease of curvature. Upstroke and peak of transmembrane voltages at the front of early excitation were influenced by the stimulus (e.g. Fig. 3a, voltage course for $0\ mm$). In the last phase of spread, when the front is near to the left end, increasing peaks of action voltages were found (e.g. Fig. 3a and b, voltage course

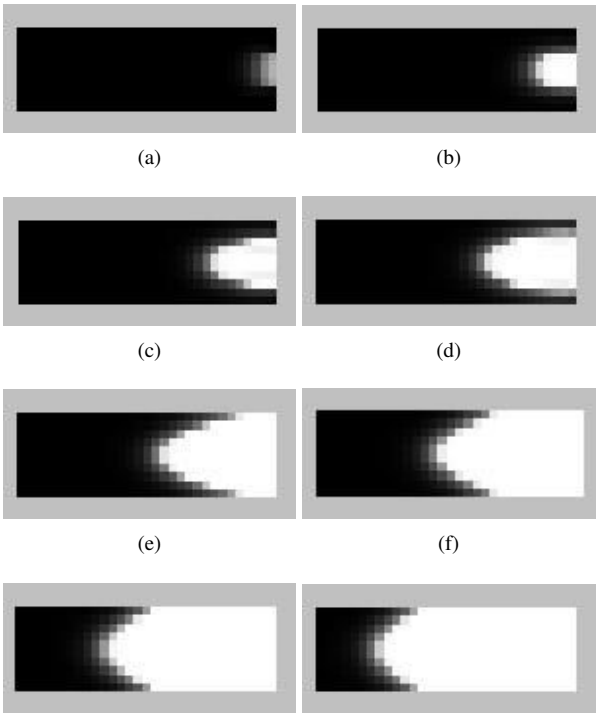

Figure 2. Transmembrane voltage in a plane through papillary muscle. A stimulus was given at time $0.5\ ms$ at the muscle's right end. The stimulus length was $1\ ms$. (a, b, ..., h) The voltage distributions are shown at $1,\ 2,\ \ldots,\ 8\ ms$. The voltages is color-coded with dark resting regions and bright activated regions.

for $2.7\ mm$), which can be attributed to reduced sinks provided by neighboring cells.

Exemplary extracellular electrograms in the bath show a typical stimulus artifact followed by changes caused by transmembrane currents (Fig. 4). The electrograms are of significantly smaller amplitude and steepness than transmembrane voltages.

Activation times at different positions were detected from the extracellular and transmembrane voltages (Fig. 5). The activation times detected in transmembrane voltages for central and surface positions indicated curvature of the activation front and boundary effects. A significant initial difference of $\approx\ 3\ ms$ is found, which is followed be a decrease to $\approx\ 0.5\ ms$. Similarly, radial differences were visible in the extracellularly detected activation times. In general, the relationship of activation time and distance was found to be nonlinear particularly at the left and right end of the preparations.

4. Conclusions

The study revealed that geometrical relationships play an important role for detection of activation times. Curvature of the wave front, particularly near

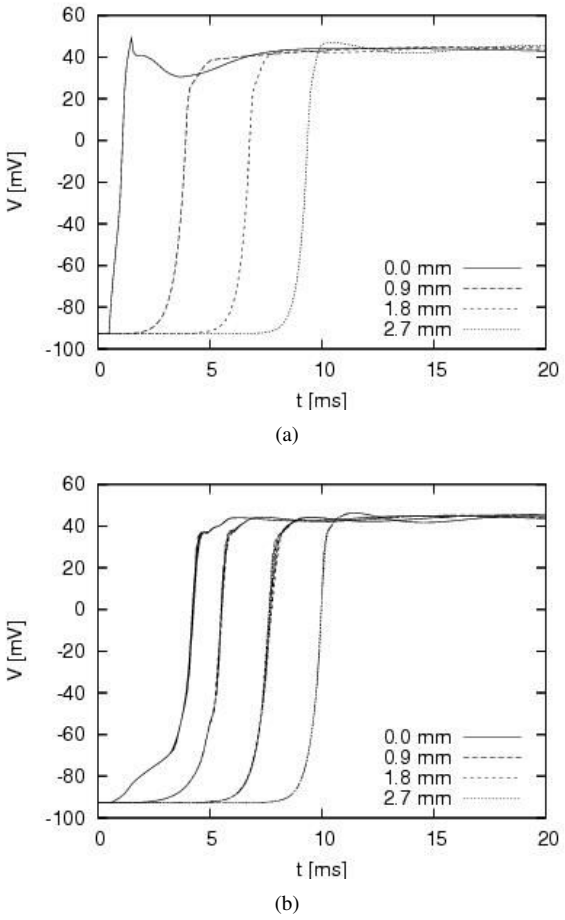

Figure 3. Transmembrane voltage at (a) central and (b) superficial positions in papillary muscle. Positions at a distance dz of 0.0, 0.9, 1.8, and $2.7\ mm$ to the right end of the muscle are shown.

to the stimulus site, led to radial differences of the transmembrane voltage and related activation times. These radial inhomogeneities of transmembrane voltage led to radial inhomogeneities of electrical fields in the bath and differences of therein activation times. Thus, particularly at the ends of the preparation the linearity of the relationship of activation time and distance degrades significantly as the distance of measurement position to the preparation increases.

In this study, the curvature of the wave front was convex resulting from the stimulus applied at the center of the right face of the muscle. Another study reported a concave curvature for a cylindrical strand of cardiac muscle [7]. The differences can be explained by the varying geometry of muscle as well as type and location of stimulus electrodes. In future studies a more realistic, superficial stimulus electrode location will be investigated.

The study indicates that conduction velocity can be detected with a given accuracy only in a specific area,

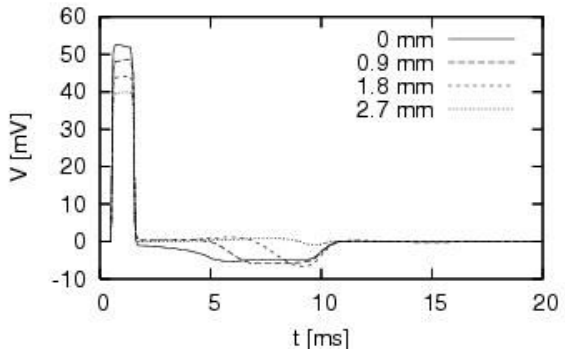

(a)

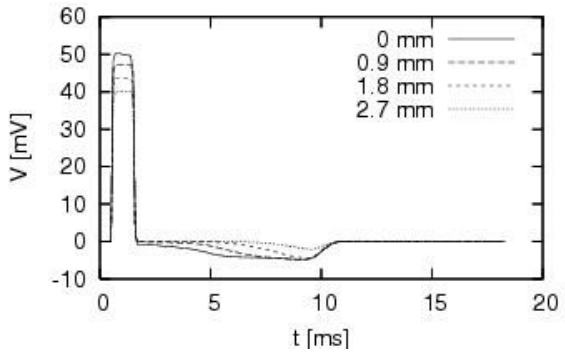

(b)

Figure 4. Extracellular potentials in bath at different positions. The positions have a radial distance of (a) 0.3 and (b) 0.9 mm to the surface of papillary muscle as well as a distance dz of 0 - 2.7 mm to a plane through the right end of the muscle.

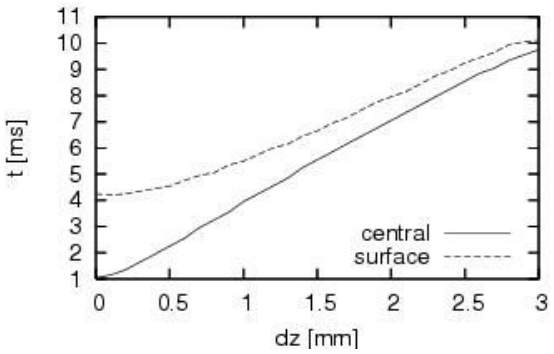

(a)

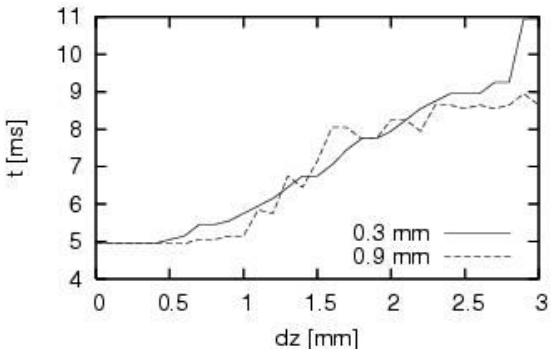

(b)

Figure 5. Detected activation times at distances dz of 0 - 3 mm to a plane through the right end of the muscle. The activations times are determined (a) at central and superficial positions from transmembrane voltages and (b) at positions in a distance of 0.3 and 0.9 mm to the muscle surface from potentials in the bath.

which is defined by geometrical relationships. The chosen computer-based modeling approach proved to reduce complexity in answering this study's question, particularly in comparison to experimental animal studies.

Acknowledgments

This work has been supported by the Richard A. and Nora Eccles Fund for Cardiovascular Research and awards from the Nora Eccles Treadwell Foundation. The authors gratefully acknowledge computing resources kindly provided by the Scientific Computing and Imaging Institute and the NIH NCRR Center for Bioelectric Field Modeling, Simulation, and Visualization.

References

[1] Sachse FB, Steadman BW, Bridge JHB, Punske BB, Taccardi B. Conduction velocity in myocardium modulated by strain: Measurement instrumentation and initial results. In Proc. 26th Conference of the IEEE EMBS. 2004; .

[2] Schwarz HR. Methode der finiten Elemente. 3 edition. Stuttgart: Teubner, 1991. ISBN 3-519-22349-X.

[3] Sachse FB. Computational Cardiology: Modeling of Anatomy, Electrophysiology, and Mechanics. LNCS 2966. Berlin, Heidelberg, New York: Springer, 2004.

[4] Noble D, Varghese A, Kohl P, Noble P. Improved guinea-pig ventricular cell model incorporating a diadic space, I_{Kr} and I_{Ks}, and length- and tension-dependend processes. Can J Cardiol Jan. 1998;14(1):123–134.

[5] Spach MS, Barr RC, Serwer GA, Kootsey JM, Johnson EA. Extracellular potentials related to intracellular action potentials in the dog purkinje system. Circ Res 1972; 30(5):505–519.

[6] Punske BB, Ni Q, Lux RL, MacLeod RS, Ershler PR, Dustman TJ, Allison MJ, Taccardi B. Spatial methods of epicardial activation time determination in normal hearts. Annals Biomed Eng 2003;31:781–792.

[7] Roth BJ. Action potential propagation in a thick strand of cardiac muscle. Circ Res 1991;68:162–173.

Address for correspondence:

PD Dr.-Ing. F. B. Sachse

Nora Eccles Harrison Cardiovascular Research and Training Institute

University of Utah, Salt Lake City, Utah, USA

E-mail: fs@cvrti.utah.edu